Int J Clin Exp Med 2017;10(5):8481-8491
www.ijcem.com /ISSN:1940-5901/IJCEM0050123

Original Article

Selection of key genes and regulators associated with Treacher Collins syndrome based on expression profiling analysis

Miao Xu[1], Aiguo Xie[2]

[1]*Department of Plastic and Reconstructive Surgery, Xinhua Hospital, School of Medicine, Shanghai Jiao Tong University, Shanghai, China;* [2]*Department of Plastic and Reconstructive Surgery, Shanghai Ninth People's Hospital, School of Medicine, Shanghai Jiao Tong University, Shanghai, China*

Received February 5, 2017; Accepted March 17, 2017; Epub May 15, 2017; Published May 30, 2017

Abstract: Objectives: Treacher Collins syndrome (TCS) is a rare congenital craniofacial defect characterized by facial dysplasia, cleft lip and cleft palate. This study aimed to explore the pathogenesis of TCS and select the key genes and regulators associated with TCS as specific molecular targets. Methods: In this study, a dataset GSE10167 was utilized containing 3 *Tcof1+/-* mutant and 3 wide-type. Following pretreatments, the differentially expressed genes (DEGs) between *Tcof1+/-* mutant and wide-type were screened using limma package. Then, these DEGs were enriched in function and pathway clusters by DAVID online tool. The protein-protein interaction (PPI) network was constructed using STRING database and miRNA-TF-target integrated network was visualized using the iRegulon plugin of Cytoscape software. Results: Totally, 353 DEGs between *Tcof1+/-* mutant and wide-type were obtained, including 142 up-regulated genes and 211 down-regulated genes. The DEGs were significantly correlated with p53 signaling pathway. In addition, by constructing PPI network of the DEGs, 4 hub nodes were selected in the network, including *CCNG1*, *TUBB3*, *HSPD1* and *ACTG1*. Moreover, in the integrated miRNA-TF-target network, 4 hub TFs were identified including E2f2, Onecut1, Wdr83 and Zbtb14. Conclusions: DEGs such as *CCNG1*, *TUBB3*, *HSPD1*, *ACTG1* and TFs of E2f2, Onecut1, Wdr83 and Zbtb14 might be used as specific therapeutic molecular targets for TCS diagnosis. However, further experiments are still needed to confirm our results.

Keywords: Treacher Collins syndrome, differentially expressed gene, protein-protein interaction network, miRNA-TF-target integrated network

Introduction

Treacher Collins syndrome (TCS, OMIM: 154500) is a congenital craniofacial defect, which is an autosomal-dominant disease [1]. The incidence of TCS is estimated as 1/50,000, and it is characterized by facial dysplasia, cleft lip and cleft palate [2, 3]. TCS is associated with respiratory failure at birth [4]. Besides, most craniofacial deformities in their childhood and adolescence require multiple rounds of surgery to repair [5].

The most common cause of TCS is the *TCOF1* gene mutation (encoding the treacle protein) [6]. *TCOF1* is extensively expressed throughout embryos at all stages of development and the levels in the neuroepithelium and neural crest were elevated [7]. Studies have shown that inhibition of p53 (pharmacological or genetic) could partially rescue facial abnormalities. More recently, a potential new treatment, N-acetylcysteine (NAC) has been administered by intraperitoneal injection in a pregnant mother to inhibit DNA damage. The method could partially rescue the facial phenotype [8]. Recently, an alternative target for the modification of ribosome biogenesis has been developed, such as targeting deubiquitinase (DUB), which could serve as a potential treatment benefited to TCS [9].

Although the craniofacial phenotype may be alleviated by p53 inhibition or anti-oxidative therapy experiments, the definitive mechanism of human treatment is not clear. Natalie *et al.*

had analyzed the possible pairwise comparisons between the three wild-type and three *Tcof1+/-* mutant embryos, but the relationship of these differentially expressed genes (DEGs) and the protein-protein interaction (PPI) network were not studied [6]. Moreover, they did not mention miRNA data. In order to find more effective targeted therapies associated with TCS, DEGs between *Tcof1+/-* mutant and wild-type embryos were determined in our study, which were mainly concentrated in the p53 signaling pathway. Besides, a PPI network was constructed to screen associated key proteins based on the DEGs. Furthermore, a miRNA-the transcription factor (TF)-target network was visualized by Cytoscape software to predicted hub TFs. Through these comprehensive bioinformatics methods, the study aimed to explore the pathogenesis of TCS and select key genes and regulators associated with TCS as specific molecular targets.

Materials and methods

This article does not contain any studies with human participants or animals performed by any of the authors. The ethics approval is unnecessary for our study.

Affymetrix microarray data

The transcription profile of GSE10167 [6] and its annotation files were got from Gene Expression Omnibus (GEO, http://www.ncbi.nlm.nih.gov/geo/) database. In this dataset, a total of 6 samples were available, including 3 *Tcof1+/-* mutants and 3 wild-type embryos. The platform for gene expression detection was GPL1261 [Mouse430_2] Affymetrix Mouse Genome 430 2.0 Array.

Data preprocessing

The raw data in the .CEL format were preprocessed with background correction, normalization and expression calculation by affy package in R [10] (Version 1.50.0, http://www.bioconductor.org/packages/release/bioc/html/affy.html), based on robust multi-array average (RMA) algorithm [11, 12]. The annotation files of this platform were used to obtain the probe value. The probes that did not match any gene symbol were removed and if one gene corresponded to several probes, the mean value of all probes was calculated and served as the final gene expression level.

Identification of DEGs between Tcof1+/- mutant and wild-type embryos

The t-test implemented in the Linear Models for Microarray (limma) package (Version 3.10.3, http://www.bioconductor.org/packages/2.9/bioc/html/limma.html) was used to identify the DEGs between *Tcof1+/-* mutant and wild-type embryos. The genes with adjusted P value less than 0.01 were regarded as DEGs.

Functional enrichment analysis of DEGs

The Gene Ontology (GO) database [13] stores broader information of gene sets, and the Kyoto Encyclopedia of Genes and Genomes (KEGG) [14] database provides informative pathways for substantial genes. Depended on these two databases, functional enrichment analysis of DEGs was performed using the online software DAVID [15]. The adjusted P value <0.05 were chosen as cut-off for significant function or pathway category selection.

To directly visualize the function of the DEGs, the ClueGO [16] plugin (Version 2.2.6, http://apps.cytoscape.org/apps/ClueGO) of Cytoscape software [17] (Version 3.4.0) was used to draw the cross-talk of enrichment results of GO biological processes (BP) and the pathway of KEGG for up-regulated and down-regulated DEGs, respectively, with the threshold of adjusted P<0.05. The CyKEGGParser plugin [18] (Version 1.2.7, http://apps.cytoscape.org/apps/CyKEGGParser) was used to draw significantly enriched pathways.

PPI network construction

PPI analysis was performed for DEGs depended on protein information in the search tool for the retrieval of interacting genes/proteins (STRING) database [19] (Version: 10.0, http://www.string-db.org/), with required confidence level (combined score) more than 0.4 as the threshold.

The network was constructed using Cytoscape software after obtaining the PPIs of DEGs. A node in the network represents a protein encoded by a DEG. The topological properties of the nodes in the network were analyzed by CytoNCA [20] plug-in (Version 2.1.6, http://

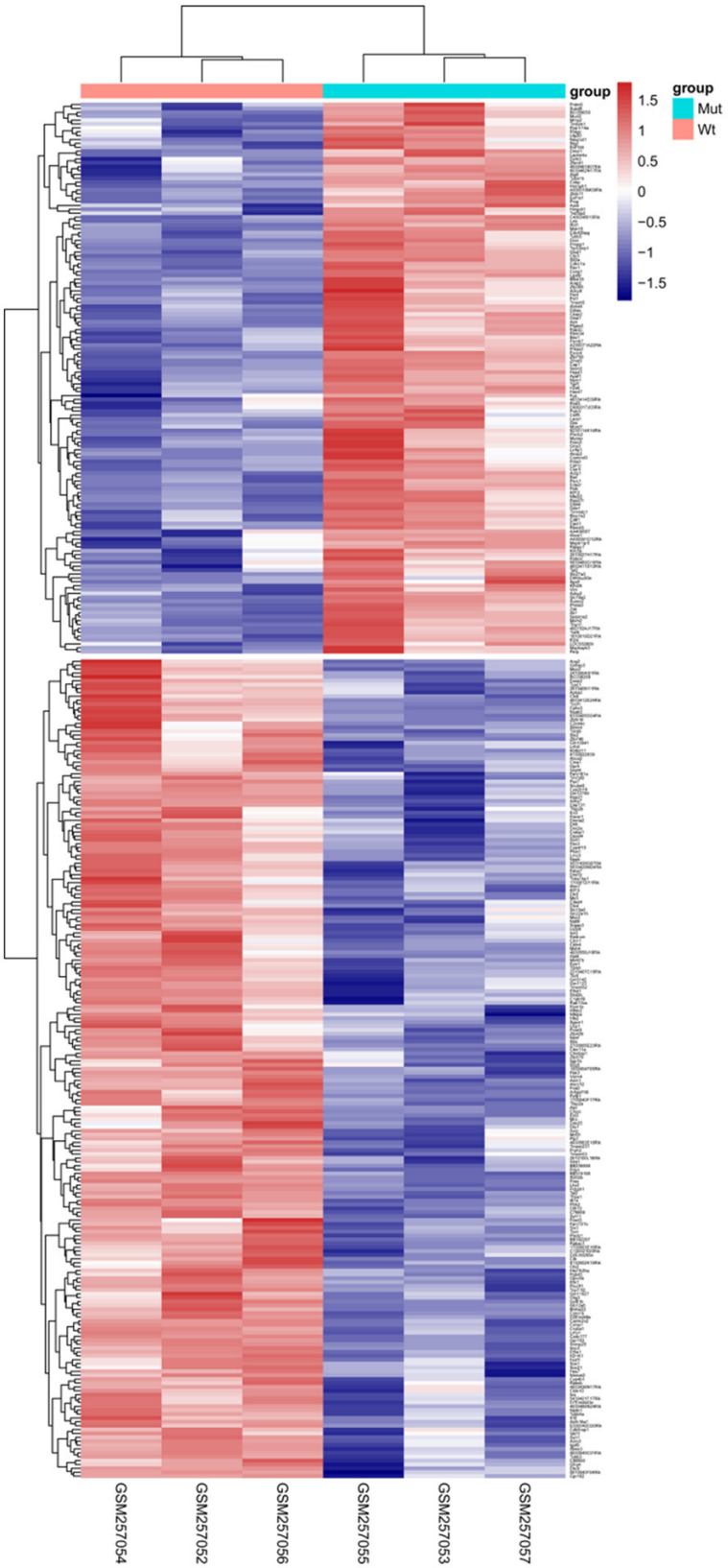

Figure 1. Two-way hierarchical clustering heat map of differentially expressed genes. The horizontal axis represents the different samples, the vertical axis represents differentially expressed genes, and the color depth represents the expression levels of the genes.

apps.cytoscape.org/apps/cytonca), and the parameter was set as "without weight". Then the Degree Centrality (DC), Betweenness centrality (BC) and Closeness centrality (CC) of the nodes were obtained. The important nodes were identified based on their ranking scores in the above three items, and were defined as hub nodes in the PPI network [21].

Prediction of TCS-associated miRNAs

The validated miRNA-target interactions in the miRWalk 2.0 (http://zmf.umm.uni-heidelberg.de/apps/zmf/mirwalk2/) database were downloaded [22, 23], and the common genes between the known targets and the DEGs were overlapped, to predict potential miRNA-target interactions related to TCS pathogenesis.

Transcription factor prediction and the construction of integrated miRNA-TF-target network

The TFs of the regulatory gene set can be predicted using the iRegulon [24] plugin (Version 1.3, http://apps.cytoscape.org/apps/iRegulon) of Cytoscape software which predicts the regulatory network by calculating the motif enrichment analysis. Based on genes in the PPI network and miRNA-target gene network, TFs of the DEGs were predicted, and the three networks were integrated to draw a miRNA-TF-target network. The topological properties of nodes in the integrated network were analyzed using the CytoNCA, with the same parameters in the PPI network analysis.

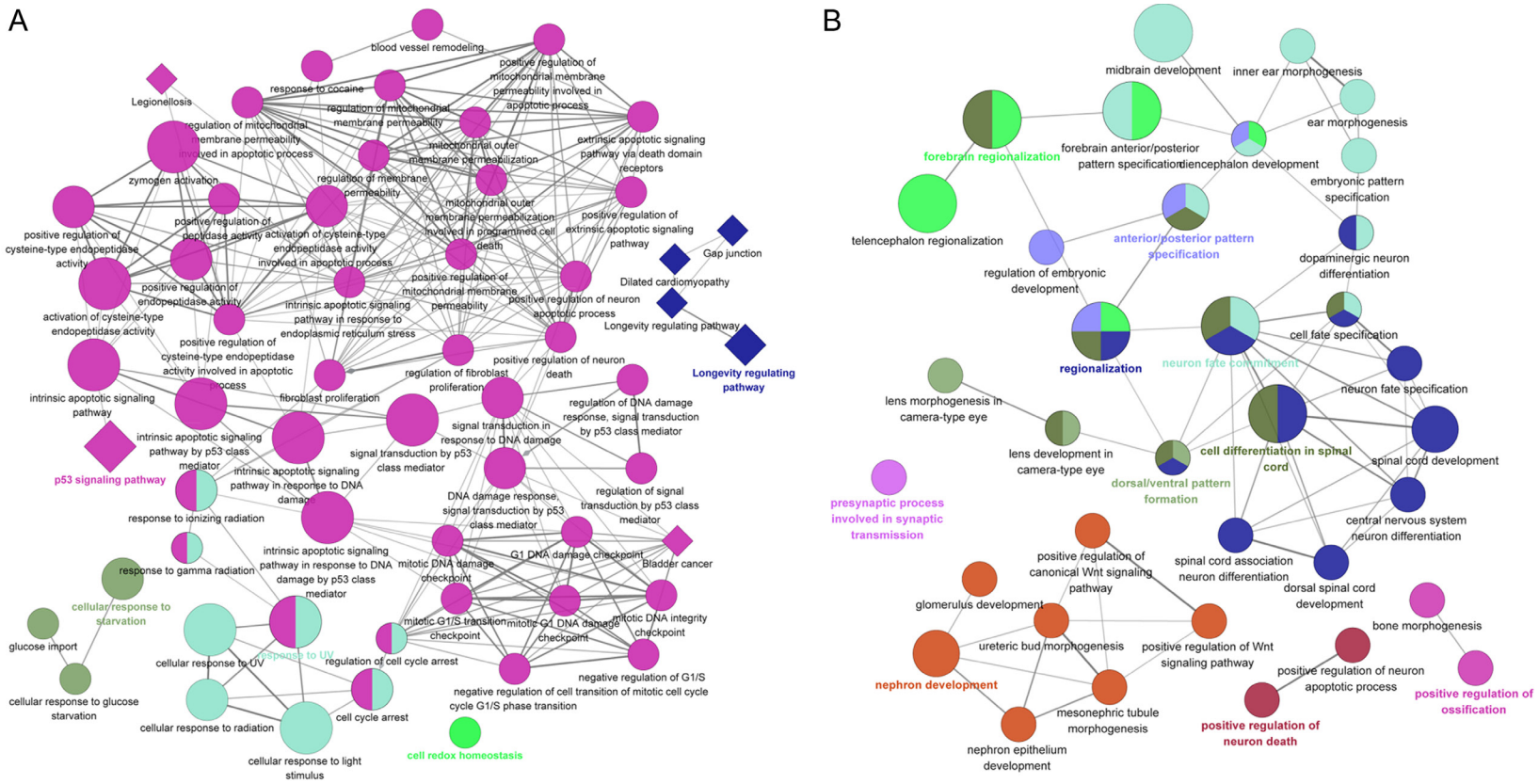

Figure 2. Cross-talk of GO functional and KEGG pathway enrichment results for up- and down-regulated DEGs. Round nodes represent GO BP categories, the diamond nodes represent the KEGG pathway categories; different color nodes represent different pathway or GO BP classifications. (A: Up-regulated, B: Down-regulated). GO: gene ontology; BP: biological process; KEGG: Kyoto Encyclopedia of Genes and Genomes.

Table 1. Top 5 significantly enriched function of up- and down-regulated DEGs

GO Terms	P-Value	Count	Genes
Up-regulated DEGs			
BP			
GO: 0042771: intrinsic apoptotic signaling pathway in response to DNA damage by p53 class mediator	3.38×10^{-5}	5	CDKN1A, AEN, RPS27L, PMAIP1, PHLDA3
GO: 0072332: intrinsic apoptotic signaling pathway by p53 class mediator	3.86×10^{-5}	5	BAX, ZMAT3, EDA2R, PMAIP1, PERP
GO: 0006974: cellular response to DNA damage stimulus	4.42×10^{-5}	12	POLK, CDKN1A, REV1, BTG2, AEN, and so on
GO: 0043065: positive regulation of apoptotic process	1.20×10^{-4}	10	ZAK, BAX, ZMAT3, TRP53INP1, NEUROD1, and so on
GO: 0006915: apoptotic process	1.55×10^{-4}	13	CKAP2, ZMAT3, FOXO3, PMAIP1, EI24, and so on
CC			
GO: 0005634: nucleus	2.95×10^{-4}	56	PTGES2, ZAK, PDIA3, ZMAT3, RPS27L, and so on
GO: 0005737: cytoplasm	4.50×10^{-4}	60	PTGES2, ADCY2, ZAK, PDIA3, FOXO3, and so on
GO: 0005829: cytosol	6.29×10^{-4}	21	EEF1A1, PAM, CNBP, PTGES2, RAP2C, and so on
GO: 0005730~nucleolus	5.91×10^{-3}	12	RBM34, EEF1A1, MAK16, ZFP750, AEN, and so on
GO: 0005881: cytoplasmic microtubule	6.20×10^{-3}	4	CKAP2, TUBA1B, GTSE1, DCXR
MF			
GO: 0000166: nucleotide binding	1.56×10^{-4}	26	RBM34, ADCY2, ZAK, ADCY8, GLUD1, and so on
GO: 0031625: ubiquitin protein ligase binding	1.04×10^{-3}	8	ACTG1, SUMO2, CDKN1A, TUBB5, MDM2, HSPD1, TUBA1B, TRAF4
GO: 0005200: structural constituent of cytoskeleton	6.17×10^{-3}	4	ACTG1, VIM, TUBB5, TUBA1B
GO: 0044822: poly(A) RNA binding	7.06×10^{-3}	15	EEF1A1, RBM34, CNBP, ZAK, PDIA3,and so on
Down-regulated DEGs			
BP			
GO: 0022037: metencephalon development	4.37×10^{-4}	3	WNT1, OTX1, OTX2
GO: 0045944: positive regulation of transcription from RNA polymerase II promoter	6.46×10^{-4}	20	LMO1, HFE2, SOX1, OTX1, OTX2, and so on
GO: 0007275: multicellular organismal development	1.01×10^{-3}	20	INA, SLC22A16, CEP131, DMRT3, OTX1, and so on
GO: 0021797: forebrain anterior/posterior pattern specification	1.08×10^{-3}	3	FEZF1, WNT1, SIX3
GO: 0043525: positive regulation of neuron apoptotic process	2.38×10^{-3}	5	PAK3, IL18, TFAP2B, TFAP2A, PCSK9
CC			
GO:0009986: cell surface	0.037	11	H2-K1, WNT1, GM1123, HFE2, STX2, STRC, PCSK9, THBS1, LRFN5, GPRC5B, ISLR2
GO: 0071547: piP-body	0.043	2	TDRD9, TDRKH
MF			
GO: 0043565: sequence-specific DNA binding	0.001	15	SOX1, OTX1, DMRT3, OTX2, SIX3, and so on
GO: 0046983: protein dimerization activity	0.002	8	TAL2, SYN1, BHLHE22, OLIG3, STX2, TFAP2B, TFAP2A, HES7
GO: 0001105: RNA polymerase II transcription coactivator activity	0.005	4	TFAP2B, TFAP2A, POU3F1, CITED4
GO: 0003677: DNA binding	0.006	27	SOX21, SOX1, DMRTA2, PAX3, ZBTB16, and so on
GO: 0005515~protein binding	0.021	53	LMO1, CROCC, PAX3, MCF2L, and so on

DEGs: differentially expressed genes; GO: Gene Ontology; BP: biological processes; CC: cell components; MF: molecular function.

Table 2. KEGG pathway enrichment analysis of DEGs

Terms	P-Value	Count	Genes
Up-regulated DEGs			
mmu04115: p53 signaling pathway	5.71×10^{-11}	11	CDKN1A, EI24, BAX, ZMAT3, MDM2, PMAIP1, APAF1, CCNG1, SESN2, PERP, GTSE1
mmu05414: Dilated cardiomyopathy	0.028	4	ACTG1, ADCY2, ADCY8, ITGA8
mmu04540: Gap junction	0.030	4	ADCY2, ADCY8, TUBB5, TUBA1B
mmu04921: Oxytocin signaling pathway	0.036	5	ACTG1, CDKN1A, ADCY2, ADCY8, PRKAA1
Down-regulated DEGs			
mmu05166: HTLV-I infection	0.033	6	H2-K1, MSX3, WNT1, ADCY7, RRAS, WNT2B
mmu05205: Proteoglycans in cancer	0.041	5	WNT1, PLCE1, RRAS, THBS1, WNT2B

KEGG: Kyoto Encyclopedia of Genes and Genomes; DEGs: differentially expressed genes.

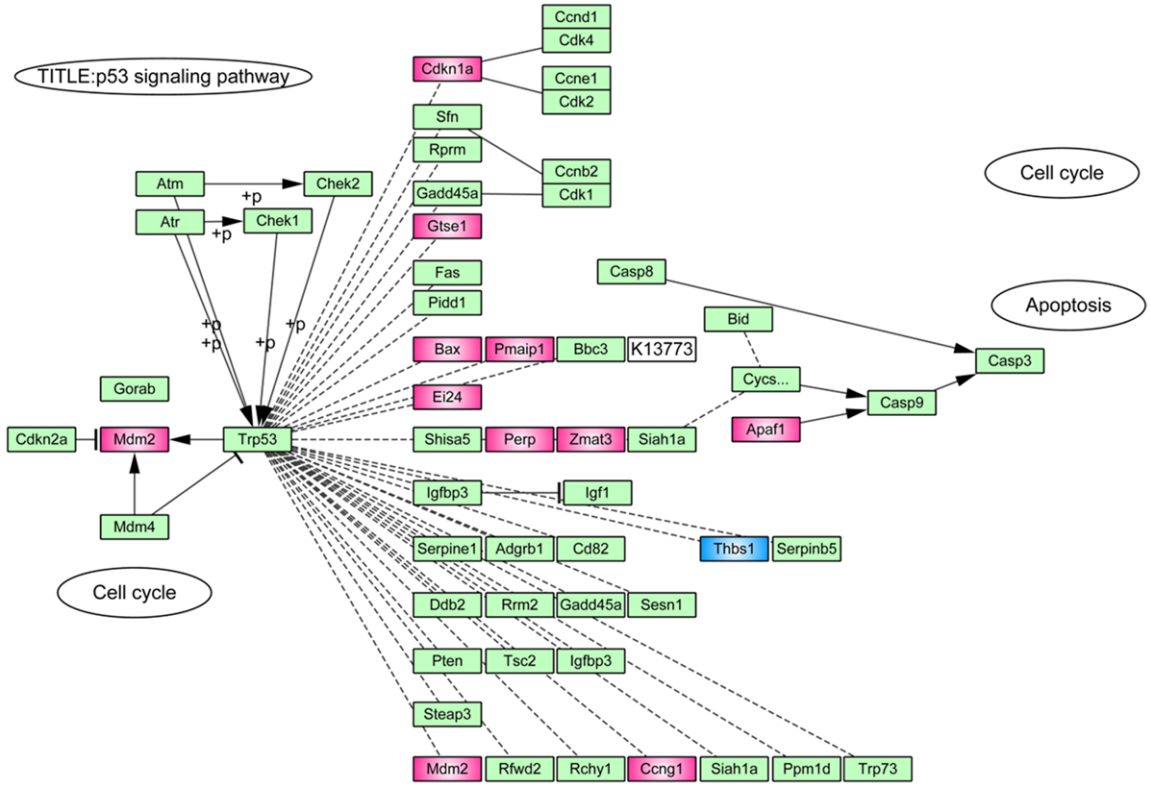

Figure 3. DEGs between *Tcof1+/-* mutant and wild-type in p53 signaling pathway. The red squares represent the up-regulated genes, the blue squares represent the down-regulated genes, the green squares represent no significant difference genes; the colorless ellipses represent the pathway names; the arrows represent activation, the T-arrows represents repression, the solid lines represent binding, dashed lines represent the state change, and "+p"s represent phosphorylation. DEGs: differentially expressed genes.

Results

DEGs screening

The dataset contained 45,101 probes, which were finally mapped to 20,708 genes after pre-treatments. Based on aforementioned criteria, a total 353 DEGs were screened out, 142 of which were up-regulated and 211 were down-regulated. Two-way hierarchical clustering heat map of DEGs were shown in **Figure 1**, and these DEGs could well distinguish the two kinds of samples.

GO function and KEGG pathway enrichment analysis of DEGs

To explore potential function and pathways for these DEGs, GO function and KEGG pathway enrichment from both up- and down-regulated DEGs were analyzed. As shown in **Figure 2**, up-regulated DEGs were mainly enriched in func-

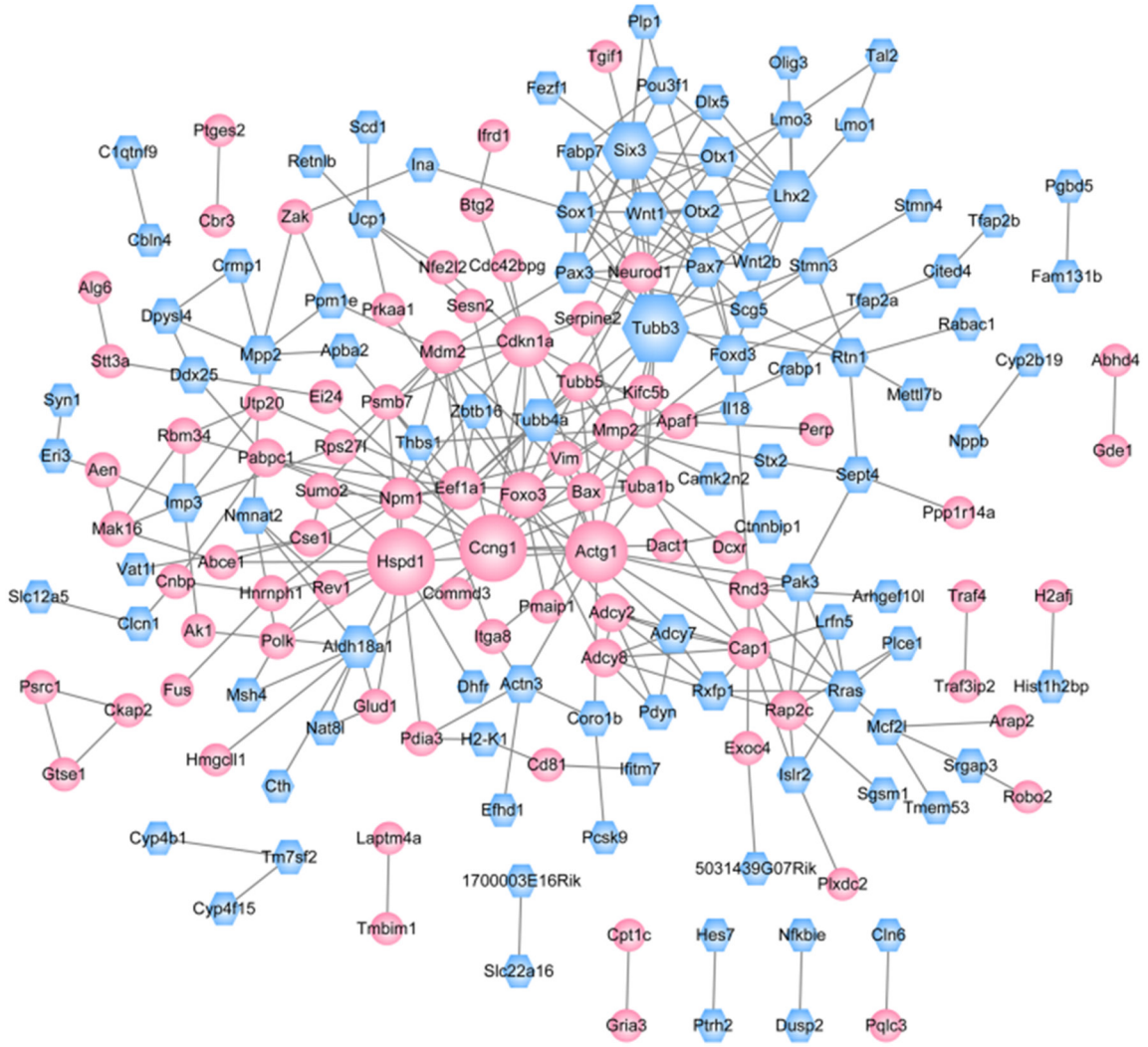

Figure 4. The PPI network of DEGs. The red circle represents the up-regulated gene, the blue polygon represents the down-regulated gene, and the node size represents the size of degree. PPI: protein-protein interaction; DEG: differentially expressed gene.

tional or pathway categories such as "regulation of cell cycle", "p53 signaling pathway (e.g. *CCNG1*)", "positive regulation of apoptotic process (e.g. *HSPD1*)", "ATP binding", "dilated cardiomyopathy and oxytocin signaling pathway (e.g. *ACTG1*)"; while down-regulated DEGs were significantly related to categories such as "protein binding", "neuron differentiation (e.g. *TUBB3*)". Top 5 (ranked by P-value) of these functional categories were shown in **Table 1**, and KEGG pathway categories were shown in **Table 2**.

Cross-talk of function and pathway enrichment results showed these DEGs were significantly associated with p53 signaling pathway. The DEGs enriched in the pathway were 11 up-regulated genes and 1 down-regulated gene (**Figure 3**).

PPI network

According to predefined criterion, a PPI network was established, containing a total of 176 nodes (including 79 up-regulated and 97 down-regulated DEGs) and 307 interactions (**Figure 4**). As shown in the PPI network, the proteins of CCNG1, TUBB3, HSPD1 and ACTG1 had high degrees (15, 15, 15, 14, respectively).

miRNA-TF-target integrated network analysis

Totally, 103 miRNA-DEG interactions were obtained based on the validated miRNA information in mice in miRWalk2.0 database, includ-

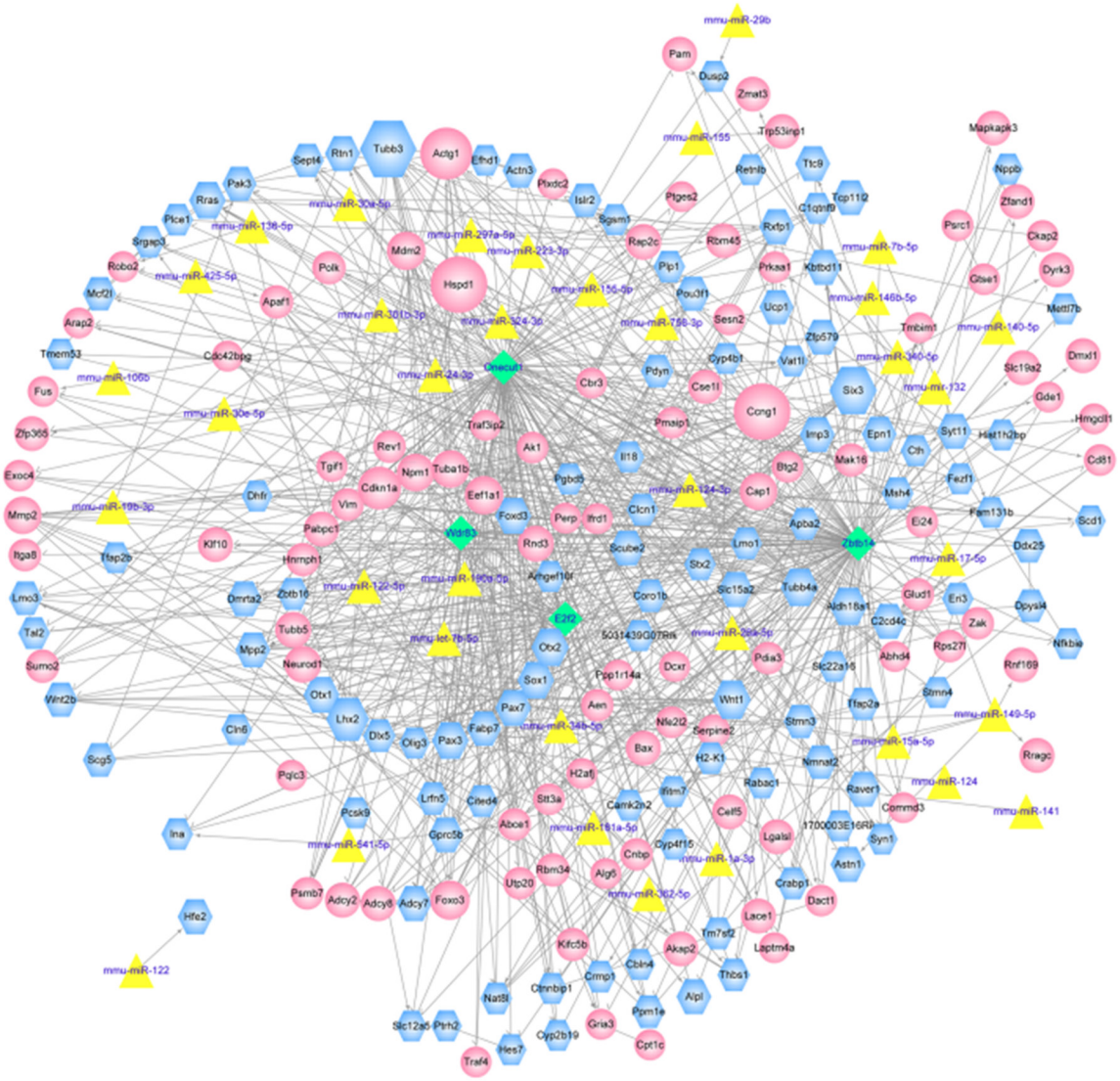

Figure 5. MiRNA-TF-target integrated regulatory network. Red circles represent up-regulated genes, blue polygons represent down-regulated genes; yellow triangles represent miRNAs, green diamonds represent transcription factors; arrowheads represent regulatory relationships, and arrowless lines represent protein interactions.

ing 36 miRNA and 103 target genes. Four TFs, such as E2f2, Onecut1, Wdr83 and Zbtb14, and their 154 target genes were predicted based on miRNA-target genes and PPI network.

By integrating the TF, DEG, miRNA information, a miRNA-TF-target network was constructed, consisted of 248 nodes (including 96 up-regulated DGEs, 112 down-regulated DEGs, 36 miRNAs and 4 TFs), 723 relationship pairs (307 PPI interactions, 103 miRNA-target interactions and 313 TF-target interactions) (**Figure 5**). And the TFs including Onecut1, Zbtb14, E2f2, and Wdr83 had high degrees (122, 114, 40, 37, respectively).

Discussion

Craniofacial malformations account for about one-third of all congenital birth defects, and TCS is a serious congenital craniofacial disease [1]. In this study, a total of 353 DEGs were obtained, including 142 up-regulated genes and 211 down-regulated genes. These DEGs were significantly correlated with p53 signaling pathway, which indicated that this pathway might play a key role in the pathogenesis of

TCS. In agreement with the previous statement, inhibition of p53 could partially rescue facial abnormities [6]. In addition, by constructing PPI network of the DEGs, 4 hub nodes were selected in the network, including *CCNG1*, *TUBB3*, *HSPD1* and *ACTG1*. Moreover, by integrating miRNA-TF-DEGs network, 4 hub TFs were identified including E2f2, Onecut1, Wdr83 and Zbtb14.

CCNG1 (CyclinG1) which has high expression level in embryonic germ (EG) and embryonic stem (ES) cells is a member of the cyclin family [25]. Transcriptional activation of *CCNG1* can be induced by tumor protein p53, and it is the only cyclin that has positive or negative effects on cell growth [26]. Previous studies have shown that *CCNG1* frequently appears in malignant tumors [25]. *TCOF1* encodes a treacle protein, which localizes to the nucleus during interphase, but disperses into the cytoplasm [27] and re-localizes at the centrosomes and kinetochores during mitosis [28]. Thus, *TCOF1* plays an important role in the process of mitosis. Besides, knockdown of *TCOF1* affects the process of mitosis, thereby interferes with the balance between expansion and differentiation of neural progenitor cells [8]. Both of *TCOF1* and *CCNG1* can affect the cell cycle. Our findings suggest that *CCNG1* is differentially expressed between *Tcof1+/-* mutant and wide-type. Thus, *CCNG1* may cause TCS by blocking the cell cycle of EG and ES.

TUBB3 encodes the beta tubulin family, which is mainly expressed in neurons, and can participate in neurogenesis, axon guidance and maintenance [29]. Treacle is typically associated with microtubule binding and it has shown that the loss of *TCOF1* will delay cell mitosis [8], and microtubules is very important in the formation of the central granule during mitosis. In our study, *TUBB3* was differentially expressed between *Tcof1+/-* mutant and wide-type, suggesting that this gene is essential for the occurrence of TCS. Precise regulation of nerve cells at specific times can prevent facial deformities. This gene may inhibit the cell cycle by altering the microtubule structure of nerve cells.

HSPD1, also known as *HSP60*, encodes a mitochondrial chaperone protein, which is a signal molecule in the innate immune system [30]. In addition to energizing cells, mitochondria are involved in processes such as cell differentiation, cell signaling, and apoptosis, as well as the ability to regulate cell growth and cell cycle progression. *TCOF1* plays an important role in the inhibition of oxidative stress-induced apoptosis, and loss of *TCOF1* results in a higher level of ROS in the body. The high level of ROS in neuroepithelium is the root cause of TCS [8]. In our study, *HSPD1* was differentially expressed between *Tcof1* mutant and wide-type, indicating that *HSPD1* plays a key role in TCS.

ACTG1 encodes γ-actin, which is one of six highly conserved actin proteins in human. It is a cytosolic actin found in the non-muscle cells, acting as a component of the cytoskeleton and a mediator of internal cellular motility [31]. This gene mutation may cause a non-syndromic hearing loss phenotype [31]. Neural crest cell formation, migration defects are considered as the basis of many craniofacial deformities. TCS is an autosomal dominant birth defect and its clinical features include damage to the middle ear and the outer ear. In our study, the differential expression of *ACTG1* which is an oxytocin signaling pathway gene was shown to play a key role in TCS.

E2f2 encodes one of the E2F family of TFs which is an important factor in controlling the cell cycle and the role of tumor suppressor proteins and is also a target for transforming proteins of small DNA tumor viruses [32]. E2f2 regulates a wide range of BPs, including cell cycle, apoptosis and DNA damage [32], which are associated with the occurrence of TCS. Consistent with it, our study also found E2f2 closely related to the DEGs between *Tcof1* mutant and wide-type. Onecut1 is responsible for the maintenance of specific cell fate and survival [33]. In our study, Onecut1 was predicted to serve as a TCS-associated TF, suggesting that Onecut1 is closely related to TCS. However, how Onecut1 works in TCS is still unknown. Wdr83 is an important module in the multicomponent stent assembly process of ERK-MAPK pathway, and abnormal activation of ERK signaling is often observed in cancer, which promotes tumorigenesis by promoting cell proliferation [34]. Increased neural crest cell proliferation is associated with decreased craniofacial defects. In our study, Wdr83 was predicted to serve as a TCS-associated TF, suggesting that Wdr83 may be closely related to TCS. Zbtb14, also known as *ZF5*, is a TF which

interacts with a GC-rich nucleotide sequences in the 5'-regulatory region of many mammalian genes [35]. ZF5 is necessary for Zn-reactive transcription [36]. This study predicted that Zbtb14 may serve as a TCS-associated TF, suggesting that Zbtb14 may relate to TCS by regulated these DGEs' expression.

In conclusion, we found that *CCNG1*, *TUBB3*, *HSPD1* and *ACTG1* may have a great influence on the progression of TCS. Besides, we also found that E2f2, Onecut1, Wdr83 and Zbtb14 may be the important TFs in the process of TCS. Thus, they may be used as specific therapeutic molecular targets for TCS prognosis. However, further experiments are still needed to confirm our results.

Disclosure of conflict of interest

None.

Address correspondence to: Aiguo Xie, Department of Plastic and Reconstructive Surgery, Shanghai Ninth People's Hospital, School of Medicine, Shanghai Jiao Tong University, 639 Zhizaoju Road, Shanghai 200011, China. Tel: +86-21-23271699-5122; E-mail: dr.aigo@aliyun.com

References

[1] Sequence AA. Positional cloning of a gene involved in the pathogenesis of Treacher Collins syndrome. The Treacher Collins syndrome collaborative group. Nat Genet 1996; 12: 130-136.

[2] Rovin S, Dachi SF, Borenstein DB and Cotter WB. Mandibulofacial dysostosis: a familial study of five generations. J Pediatr 1964; 65: 215-221.

[3] Fazen LE, Elmore J and Nadler HL. Mandibulofacial dysostosis. (Treacher-Collins syndrome). Am J Dis Child 1967; 113: 405-410.

[4] Schlump JU, Stein A, Hehr U, Karen T, Moller-Hartmann C, Elcioglu NH, Bogdanova N, Woike HF, Lohmann DR, Felderhoff-Mueser U, Linz A and Wieczorek D. Treacher Collins syndrome: clinical implications for the paediatrician-a new mutation in a severely affected newborn and comparison with three further patients with the same mutation, and review of the literature. Eur J Pediatr 2012; 171: 1611-1618.

[5] Lau MC, Kwong EM, Lai KP, Li JW, Ho JC, Chan TF, Wong CK, Jiang YJ and Tse WK. Pathogenesis of POLR1C-dependent Type 3 Treacher Collins Syndrome revealed by a zebrafish model. Biochim Biophys Acta 2016; 1862: 1147-1158.

[6] Jones NC, Lynn ML, Gaudenz K, Sakai D, Aoto K, Rey JP, Glynn EF, Ellington L, Du C, Dixon J, Dixon MJ and Trainor PA. Prevention of the neurocristopathy Treacher Collins syndrome through inhibition of p53 function. Nat Med 2008; 14: 125-133.

[7] Dixon J, Hovanes K, Shiang R and Dixon MJ. Sequence analysis, identification of evolutionary conserved motifs and expression analysis of murine tcof1 provide further evidence for a potential function for the gene and its human homologue, TCOF1. Hum Mol Genet 1997; 6: 727-737.

[8] Sakai D and Trainor PA. Face off against ROS: Tcof1/Treacle safeguards neuroepithelial cells and progenitor neural crest cells from oxidative stress during craniofacial development. Dev Growth Differ 2016; 58: 577-585.

[9] Werner A, Iwasaki S, McGourty CA, Medina-Ruiz S, Teerikorpi N, Fedrigo I, Ingolia NT and Rape M. Cell-fate determination by ubiquitin-dependent regulation of translation. Nature 2015; 525: 523-527.

[10] Gautier L, Cope L, Bolstad BM and Irizarry RA. Affy-analysis of Affymetrix GeneChip data at the probe level. Bioinformatics 2004; 20: 307-315.

[11] Bolstad BM, Irizarry RA, Astrand M and Speed TP. A comparison of normalization methods for high density oligonucleotide array data based on variance and bias. Bioinformatics 2003; 19: 185-193.

[12] Irizarry RA, Hobbs B, Collin F, Beazer-Barclay YD, Antonellis KJ, Scherf U and Speed TP. Exploration, normalization, and summaries of high density oligonucleotide array probe level data. Biostatistics 2003; 4: 249-264.

[13] Ashburner M, Ball CA, Blake JA, Botstein D, Butler H, Cherry JM, Davis AP, Dolinski K, Dwight SS, Eppig JT, Harris MA, Hill DP, Issel-Tarver L, Kasarskis A, Lewis S, Matese JC, Richardson JE, Ringwald M, Rubin GM and Sherlock G. Gene ontology: tool for the unification of biology. The Gene Ontology Consortium. Nat Genet 2000; 25: 25-29.

[14] Kanehisa M and Goto S. KEGG: kyoto encyclopedia of genes and genomes. Nucleic Acids Res 2000; 28: 27-30.

[15] Huang DW, Sherman BT, Tan Q, Collins JR, Alvord WG, Roayaei J, Stephens R, Baseler MW, Lane HC and Lempicki RA. The DAVID gene functional classification tool: a novel biological module-centric algorithm to functionally analyze large gene lists. Genome Biol 2007; 8: R183.

[16] Bindea G, Mlecnik B, Hackl H, Charoentong P, Tosolini M, Kirilovsky A, Fridman WH, Pages F, Trajanoski Z and Galon J. ClueGO: a Cytoscape plug-in to decipher functionally grouped gene ontology and pathway annotation networks. Bioinformatics 2009; 25: 1091-1093.

[17] Shannon P, Markiel A, Ozier O, Baliga NS, Wang JT, Ramage D, Amin N, Schwikowski B and Ideker T. Cytoscape: a software environment for integrated models of biomolecular interaction networks. Genome Res 2003; 13: 2498-2504.
[18] Nersisyan L, Samsonyan R and Arakelyan A. CyKEGGParser: tailoring KEGG pathways to fit into systems biology analysis workflows. F1000Res 2014; 3: 145.
[19] von Mering C, Huynen M, Jaeggi D, Schmidt S, Bork P and Snel B. STRING: a database of predicted functional associations between proteins. Nucleic Acids Res 2003; 31: 258-261.
[20] Tang Y, Li M, Wang J, Pan Y and Wu FX. CytoNCA: a cytoscape plugin for centrality analysis and evaluation of protein interaction networks. Biosystems 2015; 127: 67-72.
[21] He X and Zhang J. Why do hubs tend to be essential in protein networks? PLoS Genet 2006; 2: e88.
[22] Dweep H, Sticht C, Pandey P and Gretz N. miRWalk-database: prediction of possible miRNA binding sites by "walking" the genes of three genomes. J Biomed Inform 2011; 44: 839-847.
[23] Dweep H and Gretz N. miRWalk2.0: a comprehensive atlas of microRNA-target interactions. Nat Methods 2015; 12: 697.
[24] Janky R, Verfaillie A, Imrichova H, Van de Sande B, Standaert L, Christiaens V, Hulselmans G, Herten K, Naval Sanchez M, Potier D, Svetlichnyy D, Kalender Atak Z, Fiers M, Marine JC and Aerts S. iRegulon: from a gene list to a gene regulatory network using large motif and track collections. PLoS Comput Biol 2014; 10: e1003731.
[25] Sorrentino E, Nazzicone V, Farini D, Campagnolo L and De Felici M. Comparative transcript profiles of cell cycle-related genes in mouse primordial germ cells, embryonic stem cells and embryonic germ cells. Gene Expr Patterns 2007; 7: 714-721.
[26] Liu F, Gao X, Yu H, Yuan D, Zhang J, He Y and Yue L. Effects of expression of exogenous cyclin G1 on proliferation of human endometrial carcinoma cells. Chin J Physiol 2013; 56: 83-89.
[27] Marsh KL, Dixon J and Dixon MJ. Mutations in the Treacher Collins syndrome gene lead to mislocalization of the nucleolar protein treacle. Hum Mol Genet 1998; 7: 1795-1800.
[28] Sakai D, Dixon J, Dixon MJ and Trainor PA. Mammalian neurogenesis requires Treacle-Plk1 for precise control of spindle orientation, mitotic progression, and maintenance of neural progenitor cells. PLoS Genet 2012; 8: e1002566.
[29] Whitman MC, Andrews C, Chan WM, Tischfield MA, Stasheff SF, Brancati F, Ortiz-Gonzalez X, Nuovo S, Garaci F, MacKinnon SE, Hunter DG, Grant PE and Engle EC. Two unique TUBB3 mutations cause both CFEOM3 and malformations of cortical development. Am J Med Genet A 2016; 170A: 297-305.
[30] Landstein D, Ulmansky R and Naparstek Y. HSP60: a double edge sword in autoimmunity. Oncotarget 2015; 6: 32299-32300.
[31] Miyagawa M, Nishio SY, Ichinose A, Iwasaki S, Murata T, Kitajiri S and Usami S. Mutational spectrum and clinical features of patients with ACTG1 mutations identified by massively parallel DNA sequencing. Ann Otol Rhinol Laryngol 2015; 124 Suppl 1: 84S-93S.
[32] Chen L, Yu JH, Lu ZH and Zhang W. E2F2 induction in related to cell proliferation and poor prognosis in non-small cell lung carcinoma. Int J Clin Exp Pathol 2015; 8: 10545-10554.
[33] Espana A and Clotman F. Onecut factors control development of the Locus Coeruleus and of the mesencephalic trigeminal nucleus. Mol Cell Neurosci 2012; 50: 93-102.
[34] Lee SH, Hu LL, Gonzalez-Navajas J, Seo GS, Shen C, Brick J, Herdman S, Varki N, Corr M, Lee J and Raz E. ERK activation drives intestinal tumorigenesis in Apc(min/+) mice. Nat Med 2010; 16: 665-670.
[35] Obata T, Yanagidani A, Yokoro K, Numoto M and Yamamoto S. Analysis of the consensus binding sequence and the DNA-binding domain of ZF5. Biochem Biophys Res Commun 1999; 255: 528-534.
[36] Suzuki K, Otsuka F, Yamada H and Koizumi S. Analysis of cysteine and histidine residues required for zinc response of the transcription factor human MTF-1. Biol Pharm Bull 2015; 38: 611-617.